

This is the author's version of a manuscript that was accepted for publication in *Acta Astronautica*.

The definitive version was subsequently published in:

Fridrich Valach, Miloš Revallo, Pavel Hejda, and Josef Bochníček: Predictions of SEP events by means of a linear filter and layer-recurrent neural network.

Acta Astronautica, Volume 69, Issue 9-10, November 2011, Pages 758-766. DOI:10.1016/j.actaastro.2011.06.003

Predictions of SEP Events by Means of a Linear Filter and Layer Recurrent Neural Network

Fridrich Valach^{a,*}, Miloš Revallo^b, Pavel Hejda^c, Josef Bochníček^c

^a*Geomagnetic Observatory, Geophysical Institute, Slovak Academy of Sciences, Komárňanská 108, 947 01 Hurbanovo, Slovakia*

^b*Geophysical Institute, Slovak Academy of Sciences, Bratislava, Slovakia*

^c*Institute of Geophysics, Academy of Sciences of the Czech Republic, Prague, Czech Republic*

*Corresponding author. Tel.: +421 35 760 22 11; fax: +421 35 760 24 94.

E-mail addresses: fridrich@geomag.sk (F. Valach), geofmire@savba.sk (M. Revallo), ph@ig.cas.cz (P. Hejda), jboch@ig.cas.cz (J. Bochníček).

Abstract:

Solar energetic particle (SEP) modelling has gained great interest in the community, specifically in connection with the safety of crews and the protection of technological systems of spacecraft situated outside the shielding of Earth's magnetosphere. Two models for the prediction of SEP events are presented in this paper. The models are based on a linear filter and on a special type of dynamic artificial neural network known as the layer-recurrent neural network. In this work they use as input the following parameters: the X-ray flare class for flares originating close to the centre of the solar disk; observed type II or IV radio bursts; and of the position angle, width and linear speed of observed full or partial halo CMEs. The models are designed to provide forecasts of proton fluxes with energies exceeding 10 MeV at the L1 libration point.

Keywords: coronal mass ejection; X-ray flare; solar energetic particles; artificial neural network.

1. Introduction

Explosive and high-dynamic processes in the solar corona and interplanetary magnetized plasmas accelerate particles, such as electrons, protons, heavy ions, and neutrals up to high energies. Periods of enhanced fluxes of such particles, especially protons with energies exceeding 10 MeV, are called solar energetic particle (SEP) events. To consider SEPs in a space weather context is a matter of critical importance. SEPs are able to penetrate through the protective shielding of spaceships travelling outside the Earth's magnetosphere and can jeopardize the lives of humans on board and damage sensitive technological systems.

It is generally acknowledged that SEPs can have harmful effects not only on spacecraft but on aircraft crews and passengers, on communication systems, etc. They represent serious hazards for astronauts on missions to the Moon and Mars for example planned by NASA's "Vision for Space Exploration," e.g., if astronauts had been on some extra-vehicular activity on the Moon [1, 2, etc.]. Predicting SEP events at 1 AU, and also out further, towards the orbit of Mars, is therefore a necessary objective in the effort to minimize the dangers from SEPs to humans and systems on such missions.

The energy of SEPs ranges from a few kiloelectronvolts to several gigaelectronvolts. The fastest particles can travel with velocities of up to half the speed of light and they can reach 1 AU within 15-20 minutes after the appropriate solar event is launched. The most important places where solar particles are accelerated are regions where solar flares occurred as well as shocks in the solar corona and interplanetary space.

Recent data indicate that large SEP events are associated with fast and wide coronal mass ejections (CMEs): for a comprehensive review of the CME subject see, e.g., [3, 4, or 5]. CME-driven shocks accelerate protons, which are detected as SEP events. They also accelerate electrons, which produce type II radio bursts, being an indicator of super-Alfvenic mass motion [3]. Hwang *et al.* [1] found that there were type II radio bursts in all the largest SEP events occurring in solar cycle 23 (1997-2006). Moving type IV radio bursts are also

expected to be closely related to CMEs [3] because they indicate magnetized plasma ejection. It must be emphasized that only about one per cent of the fastest CMEs produce significant SEP events. Flares as a possible source of SEPs must be mentioned here as well. Gopalswamy [3] describes three different current viewpoints about the flare-CME relationship. The first is that flares produce CMEs [6], the second, presented by Hundhausen [7] is that flares are byproducts of CMEs and the third point of view is that flares and CMEs are part of the same magnetic eruption process [8, 9].

In connection with space weather, we must state that direct injections of impulsive SEPs, which are believed to be connected with flares, affect only narrow parts of space. The impulsive events have typical durations of the order of hours and are less intense than gradual events which can last several days [10]. Only CME-driven shocks can spread to large parts of space and flood them with high fluxes of SEPs [11, 12, and 13].

On the other hand, some authors [14] prefer flare information (X-ray flares) as a basis for proton event forecasting. X-ray classes (intensities of X-ray flares) together with information about their positions on the solar disk (H-alpha flare positions) and accompanying type II and/or IV bursts has been found to be good input parameters also when the geomagnetic activity is being forecast [15, 16].

It appears to be correct that both CME and flare information are of great importance for the forecasting of large SEP events.

It was found that the efficiency of particle acceleration is enhanced when the primary CME runs into regions of enhanced density due to preceding CMEs or streamers [17, 1]. Thus both impulsive flares and preceding CMEs may serve as sources of the seed particles for SEPs accelerated by the following CME. Their effects on SEPs are similar [1].

In addition to the presence of seed particles, the physical conditions in the ambient medium can modify the characteristics of the shocks and hence affect the intensity of SEPs [1, 18]. Hwang *et al.* [1] investigated SEP events of solar cycle 23 in detail. They found some special

properties of extremely large SEP events for which proton peak intensity was over 10^4 pfu = 10^4 protons/cm².s.sr in the > 10 MeV channel of the GOES instrument. All of them were associated with very fast halo CMEs (> 1400 km/s), and, except for one event, these large events were located at the disk centre within a latitude strip between N22 and S16, and longitude band between W34 and E23. All together six extremely large SEP events occurred during solar cycle 23.

Studying SEP events for intensity > 10 pfu (which is usually considered the threshold for SEP events), Hwang *et al.* [1] found a tendency that CME speed is related to the SEP time scales (e.g., duration time of a SEP event). On the other hand, SEP peak intensity depends on the Earthward direction parameter of the CME, which is a parameter quantifying symmetric characteristics of the shape of the CME [19], together with the X-ray strength [1]. The statistical properties of SEPs concerning their time scales as well as intensities were studied in [20] in the frame of the ESA SEP-EM Project.

In order to study SEP events a modern powerful tool of advanced statistics is required. Artificial neural networks can be the possible choice to accomplish this task. A relevant definition of a neural network (NN) which describes the subject very well can be found in [21]: “A Neural Network is an interconnected assembly of single processing elements, units or nodes, whose functionality is loosely based on the animal neuron. The processing ability of the network is stored in the interunit connection strengths, or weights, obtained by a process of adaptation to, or learning from, a set of training patterns.” NNs have been trained to perform complex functions in various fields, including pattern recognition, identification, classification, speech, vision, and control systems. Today NNs can be trained to solve problems that are difficult for conventional computers or human beings [22]. They have been used in space weather studies, too [e.g., 16].

The aim of this paper is to forecast and study SEP events, especially large ones, using artificial neural networks. Input parameters are chosen to be both solar flare and CME parameters. In large SEP events it is apparent that the way in which SEPs are accelerated by a CME depends not only on the parameters of the CME in question. The preceding CMEs

and/or flares that occurred in the same regions have to be taken into consideration as well. That is why we believe that special types of artificial neural networks can be helpful tools for SEP forecasting. Dynamic networks can cope with temporal structures in studied time series. For that reason we expect them to be particularly effective for the purpose of our study. Section 2 introduces the data used, as well as the methods of modelling based on several kinds of NNs. The results of the study are presented and discussed in Section 3. The main findings are summarised in Section 4.

2 Materials and methods

2.1 Data used

For SEP event modelling we considered information characterising CMEs to be important input parameters. Only full and partial halo CMEs were used in our study; for partial halo CMEs, only those with a width exceeding 140° . Three characteristics of the full/partial halo CMEs were considered: (1.) Position Angle (PA) measured from Solar North in degrees (counter-clockwise); (2.) Width; (3.) Linear Speed.

The Large Angle Spectrometric Coronagraph (LASCO) on board SOHO has been providing unprecedented views of the solar corona since January 1996. In the beginning, this instrument contained three individual coronagraphs C1, C2, and C3. However, the C1 was disabled in June 1998. C2 and C3 are white light coronagraphs imaging from 2 to 6 solar radii and from 3.7 to 32 solar radii, respectively. Data which we used were taken from [23]. The SOHO/LASCO CME Catalog is available here [4]. The Catalog is generated and maintained at the CDAW Data Center by NASA and The Catholic University of America in cooperation with the Naval Research Laboratory.

Additional information used in our study concerned solar flares. We were interested in the X-ray flares which were observed near the centre of the solar disk (up to $\pm 40^\circ$ in heliographic longitude and latitude) and were accompanied with radio bursts of types II or IV. The class of

X-ray flare (XRA Class) was the quantity which was taken as an input parameter [24]. The data were taken from daily bulletins issued by the NOAA Space Environment Center, Boulder, Colorado, USA [25].

The quantity which we intended to model was the SEP flux represented by the flux of high-energy protons (HEPF) with energies over 10 MeV. The SEP data are from the Solar Isotope Spectrometer on the ACE Satellite. We have used data prepared and issued daily by the NOAA Space Environment Center (files YYYYMMDD_ace_sis_5m.txt) [26]. Daily values were averaged from 5 minute values published in the daily reports.

For this study we focused on the years 1998-2005. The reason is the frequency of CME occurrence. During these solar maximum years full or partial halo CMEs appeared frequently, approximately one event every 36 hours.

2.2 Patterns for neural networks

Daily characteristics of CMEs, solar flares and SEPs were used in the modelling. The characteristics of CMEs and flares were used as input parameters to the neural network models. SEP characteristics were used as output parameters.

For SEPs (HEPF) the daily mean values were computed in a simple way as the average value of HEPF>10MeV throughout the day. There were, however, some gaps in data sets. Therefore, for some days the mean values had to be computed using incomplete data. In these instances the means were computed using all available data. At times there were data gaps covering several days. Fortunately, they fell within the periods when no significant enhancements of SEP fluxes occurred; we deduced this overlooking the data of the previous and following days, respectively. In these cases the interpolated values based on the previous and following daily mean values of HEPF were adopted. Inspecting the GOES proton data [27] we confirmed that no considerable SEP event has been omitted from our data base.

A more complicated task was preparing the daily characteristics of the CMEs and flares. This was due to there being days when neither halo CME nor significant flare occurred. On the other hand, there were also days when two or more of such events occurred. We solved the problem in the following way.

We established four pieces of information about full or partial halo CMEs on a given day as input parameters for our neural network models:

1. The position angle of the most important CME. If more than one CME occurred, the one with the greater width was considered to be more important. The position angle is not given for full halo CMEs; in such cases the value -360 is taken as the model input.
2. The greatest width of the CME which was observed on a given day.
3. The linear speed of the most important CME (the one with the greater width was considered to be more important).
4. The number of CMEs which were observed during a given day.

If no halo CME was observed during the day, these four parameters were set to 0 (zero).

We also established four pieces of information about X-ray flares (XRAs) on a given day as input parameters for our neural network models:

1. The class of the most important X-ray flare (XRA class) which was observed close to the centre of the solar disk ($\pm 40^\circ$).
2. Information about the type II radio burst (RPS II) accompanying the X-ray flare. The value is set to 1 or 0 if RPS II was or was not observed, respectively.
3. Information about the type IV radio burst (RPS IV) accompanying the X-ray flare. The value is set to 1 or 0 if RPS IV was or was not observed, respectively.
4. The number of X-ray flares which were observed close to the centre of the solar disk.

If no flare was observed during the day, these four parameters were set to 0 (zero).

The decision about which flare is the most important (if there were more than one XRA close to the centre of solar disk) was made according to the conclusions made by [15, 16] for

geomagnetic activity forecast purposes. The first criterion was information about RSP IV; the most important flare event was often found to be accompanied by it. If this criterion did not help us to decide, then we took a decision in regard to the XRA classes; the higher the class the more important the XRA. Only if these two criteria failed did we resolve the issue according to the information about RSP II so that the most important XRA was accompanied by it. As an illustrative example, let us consider six XRAs of class B or stronger which occurred near the solar disk centre on October 29, 2003. However, only those accompanied by RSP II and/or RSP IV are interesting for this study. There were two such events on that day:

- XRA of class M3 accompanied by RSP IV
- XRA of class X1 accompanied by both RSP II and RSP IV

Which of them is of most importance for our study? The first criterion states that the events accompanied by RSP IV are more important than those without RSP IV. Thus the first criterion does not answer the question. Therefore we have to compare the XRA classes of the events (second criterion). The XRA with the X1 class is chosen to be the most important event of the day. In a hypothetical case if even the XRA classes are equal, the most important event would then be the one accompanied by RSP II (third criterion).

2.3 Neural network models

The definition of an artificial neural network (NN) is introduced at the end of Section 1. There are many specialized software products which can interface with NN's. For the purposes of this paper Matlab software was used with its Neural Network Toolbox 5 [22].

After the gaps from the data sequence were removed, a quasi-continuous sequence of 1978 patterns was at our disposal. Handling the neural networks one usually needs to have three segregated sets of patterns: 1. those intended for the training process (training patterns), 2. those dedicated to estimating an optimal architecture of the network and the training parameters (so-called validation patterns), and 3. those reserved for some final tests (final test patterns). Schmid [28] suggests that the whole set of patterns has to be split to the training,

validation, and final-test subsets in proportion 3 : 1 : 2, respectively. We divided the sequence of patterns in such a way that the three subsets contain the cases of the most significant HEPF enhancements distributed according to the required proportion. First 480 patterns were assigned to the validation, then 740 patterns were allocated for training, and finally 758 patterns were custom made to the independent final test.

In the following, four NN models are considered and their results are presented. Section 2.3.1 introduces two models based on linear filters. In Section 2.3.2, a more advanced model of the NN is adopted where a new layer of so-called hidden neurons is added to the network architecture. A more sophisticated NN model based on recurrent network is dealt with in Section 2.3.3.

2.3.1 Linear filters

Linear filters were the simplest neural network models which we employed. They represent a class of neural network without so-called hidden neurons [21, 22]. This fact disables them to solve linearly non-separable problems [21], which is a drawback. However, their advantage consists in their simplicity. The networks were fed by the aforementioned eight input parameters concerning CMEs and XRAs. The model was trained to provide one-step-ahead predictions of HEPF > 10 MeV. That means that the predictions based on the data from the previous 24-hour interval were directed immediately at the succeeding 24-hour interval.

First the training was set up to use training patterns. In so doing we compared the results obtained involving a different history of input parameters. This means that beside the data from the previous 24-hour interval we also tried to involve older data about CMEs and XRAs, specifically, we also tried to include the data of 0, 1, 2, ..., and of 12 previous days. In this way the linear filter became a dynamic linear filter. The performances of the 13 models on the validation patterns were compared with each other.

The quality of the linear-filter models as a function of the history length of input parameters was investigated on validation patterns. The method of quality classification was a simple subjective estimation in the course of comparing the graphs with each other. It turned out that

the best results were obtained for the plainest model, which did not consider more data from previous days. Together with this best linear model there was also a model including eight more previous days' data as inputs. We deemed these two networks to be the best – a linear filter without history (LF0) and a linear filter with an 8-day history (LF8). So as to utilize the maximum information contained in both validation and training patterns, we executed the training for LF0 and LF8 again utilizing a joint set of patterns comprised of both validation and training patterns.

2.3.2 Neural network with hidden neurons

Neural network with hidden neurons (HNN) is a higher level of artificial neural networks. Hidden neurons enable the network to solve the linearly non-separable class of problems [21]. The training process is numerically much more complicated than that of linear filters. Here we had three unknown parameters of an optimal neural network instead of one (compared with linear filters where there was only one unknown parameter, i.e., the history of inputs). We had to find an optimal length of history which must be included with the input of the model; we had to do it because from the linear filtering no definite answer arose. In addition, we had to estimate the proper number of hidden neurons as well as an optimal number of training epochs (for a more detailed explanation, see e.g., [21, 22, and 28]). The procedures for searching the optimal parameters were similar to those made for linear filters but in this case we trained 990 neural networks. The history was changed from 0 to 8 (which came from the results of the linear filters), the number of hidden neurons varied from 2 to 12, and we tried 10 different numbers of training epochs ranging from 5 to 200.

From the test on the validation patterns we learned that the optimal parameters of the neural network with one hidden layer are as follows: (1) A history of input parameters (information about CMEs and XRAs) has to include six days beside the data from the previous 24-hour interval. (2) Two neurons on the hidden layer are sufficient. (3) The training process has to be suspended after 15 epochs if trained on the set labelled as training patterns in the above text.

These optimal parameters were adopted for the new neural network model. We used the joint set of patterns comprised of both validation and training patterns for the new training process. Because the new set of patterns employed for training consists of more patterns than were in the old set, the number of training epochs was adjusted properly so as to avoid an overfitting; 12 epochs were run instead of 15. Because the result of the training processes for this kind of network depends a little on the initial values of the weights (they are set randomly at the beginning of the training process), we trained 11 networks instead of a single one. As a model, output medians of the 11 NN's were considered.

2.3.3 Recurrent network

The recurrent network can be regarded to be an advanced neural network with a hidden layer. Some structures are incorporated in the architecture of the network which makes it possible to deal with the history of input parameters beside their actual values [21]. There is no need to search for an optimal length of the history, as required in the previous procedures. However, the training process takes much longer than the training of an ordinary neural network [22]. We needed to find the optimal number of hidden neurons and the number of training epochs. This procedure followed the previous ones. All together 105 NN's were trained on the training patterns, the number of hidden neurons changing from 2 to 10, while the numbers of training epochs were in the range of 10 to 50. The optimal NN's parameters were estimated on validation patterns which are two neurons in the hidden layer and 12 training epochs.

The estimated optimal parameters were adopted for the new recurrent network (RNN) model. Again we used the joint set of patterns comprised of both validation and training patterns for the new training process. The number of training epochs was reduced to nine. Because of the slight influence of the initial values of the weights, we trained 11 networks and medians of the 11 NN's were considered as a final output.

3 Results and discussion

All results presented in this section were computed for the final test patterns, labelled as such in the above text. These patterns were used neither in the training process nor for validation. Therefore the final test is considered to be independent. The question about the model accuracy can be addressed when a real practical use is simulated. Here we proposed two recipes on how the models could be used in practice, followed by a summary of successes and failures.

We imagined a situation of how our models would be used if a spacecraft travelling outside the Earth's magnetosphere had to perform safety measures against SEP events. One example is whether or not an astronaut could be sent into free space outside the protected spacecraft. For this example we examined two different levels of safety measures which we named Recipe A and Recipe B, respectively.

Recipe A is the simple instruction for performing safety measures if a critical level of HEPF forecast is exceeded during the following 24 hours from a given start time.

Recipe B is a more careful plan. The safety measure is imposed for the ensuing 24 hours when the models forecast an overload of the critical HEPF level during the 24-hour interval. This also applies when the overload was forecast for the previous 24-hour interval (whether it took place or not), and also if the overloaded HEPF was observed during the previous 24 hours. For both the successive 24-hour intervals, the same critical level of HEPF is prescribed.

Some statistics comparing the success of the four NN models presented in the previous Section (LF0, LF8, HNN, and RNN) for Recipes A and B are listed in **Table 1**. The models were run over the test period 13/08/2003 – 26/11/2005. Critical levels of HEPF were set to be 100, 200, 500, and 1000 pfu.

Surprisingly, the most convincing results appeared to be obtained when the plainest NN model, i.e., linear filter fed with the CME and XRA information of the past 24-hour interval, was employed (**Figure 1** and for more details see also **Figure 2**). However, more detailed scrutiny of the results (**Table 1**) reveals that the good score of the days with SEP events when a safety measure was performed are at the expense of the rate of days when the safety measure was not performed. On the other hand, the recurrent network provides the forecasts (**Figures 1 and 2**) which lead to the smallest waste of time with some “feasible” hazard (**Table 1**).

A compromise between “too cautious” LF0 and “saving-time” RNN models can be achieved by averaging their outputs. The statistics of such a combined model (LF0-RNN) seems to be the most satisfying (**Table 2**).

It must be noted that Recipe B is the more convenient instruction for practical demands than Recipe A. It can be explained by the time resolution of the day-long data used in the study.

Moreover, present conditions suggest the danger could also continue the following day. Hence adopting such an intuitive consideration to the instruction (Recipe B) could increase the safety of crews and technical equipment of spacecraft.

Some papers (e.g., [29]) define SEP events to be the enhancements of HEPF which represent the critical level of the flux equal to about 10 pfu. In this sense the models proposed here are intended to be restricted only to large SEP events. The noise which spoils the model outputs is of a level comparable to or exceeding 10 pfu.

In order to be able to compare our results with some standard, we calculated (the last columns in **Tables 1 and 2**) the Hanssen-Kuiper skill score (*KSS*), known also as true skill statistic (*TSS*). It is defined by the formula

$$KSS = (ad - bc) / [(a + c)(b + d)],$$

where *a* is the number of hits (correctly forecast SEP events), *b* is the number of false alarms, *c* is the number of missing alerts, and *d* is the number of correct non-event forecasts. The

This is the author's version of a manuscript that was accepted for publication in *Acta Astronautica*.

The definitive version was subsequently published in:

Fridrich Valach, Miloš Revallo, Pavel Hejda, and Josef Bochníček: Predictions of SEP events by means of a linear filter and layer-recurrent neural network.

Acta Astronautica, Volume 69, Issue 9-10, November 2011, Pages 758-766. DOI:10.1016/j.actaastro.2011.06.003

values of *KSS* range from -1 to 1. Value 1 means a perfect score while value 0 stands for no skill level.

The values of *KSS* were calculated for the test period 13/08/2003 – 26/11/2005. With the combined model LF0-RNN and the Recipe B employed, *KSS* equals 0.66, 0.87, 0.72, and 0.45 for SEP threshold values 100 pfu, 200 pfu, 500 pfu, and 1000 pfu, respectively (**Table 2**). First three of these values seem to be better than $KSS = 0.54$ which can be calculated for the forecasts of SEP events referred by Kahler et al. [29]. It has to be reminded, however, that Kahler et al. [29] dealt with SEP events defined with threshold value 10 pfu, while we studied much stronger events in this paper.

In the data sets used for the input data preparation many gaps were present. Sometimes the gaps overran one or more days. This is an unpleasant fact when using dynamic neural networks where one relies on continuous data sequences. We were forced to bridge the gaps each time a gap exceeded one day. This one-day critical threshold was chosen because CMEs occurred with the frequency of approximately one event every 36 hours. In such a manner the corruption of the time series for the dynamic neural networks is quite tolerable if it does not appear too often. In the opposite instance, many discontinuities would constitute a disturbance and hence a problem for dynamic networks.

One more interesting feature of the NN's with hidden layers, which appeared to be the best (HNN, RNN), is that these layers consist of only two neurons. It might indicate that the relations among the studied CME, XRA, and SEP parameters are not too complicated, however, it might also arise from contradictory data in some cases.

4 Conclusions

The work that has been presented is based on four neural network models:

- LF0 (Linear filter without history)
- LF8 (Linear filter with an 8-day history)
- HNN (Neural network with hidden neurons)
- RNN (Recurrent neural network)

This is the author's version of a manuscript that was accepted for publication in *Acta Astronautica*.

The definitive version was subsequently published in:

Fridrich Valach, Miloš Revallo, Pavel Hejda, and Josef Bochníček: Predictions of SEP events by means of a linear filter and layer-recurrent neural network.

Acta Astronautica, Volume 69, Issue 9-10, November 2011, Pages 758-766. DOI:10.1016/j.actaastro.2011.06.003

The final model, LF0-RNN, combining the linear filter fed with CME and XRA information obtained during the previous 24-hour interval and the layer-recurrent neural network fed with the sequence of the same information proved to be the best way to forecast severe SEP events.

We propose to issue an alert for a succeeding 24 hour period if the model forecasts an overload of the critical HEPF level during that period, as well as when the overload was forecast for the previous 24-hour interval, and also if the overloaded HEPF was observed during the stated interval.

If the critical level of HEPF was set to be 100 pfu, 28 SEP events were foreseen in time out of the 34 SEP total events occurring during the test period. It was carried off at the toll of 116 false alarms. In doing so, the rate of days when the safety measure was performed constituted 19% of all the tested days. The results obtained were still more encouraging when the critical level of HEPF was heightened to 200 pfu.

In this study, the prediction of SEP events has been performed, with focus on continuous time series rather than single solar SEP events. As for the single events approach, there can be difficulties to distinguish between the response of particular solar energetic particle events in case of their successive emergence. The response of interplanetary medium can be complicated by its "memory" effects, and therefore the forecast of SEP events should rely not only on current solar event data but should also consider the influence of past SEP data records. In this study, we attempted to make a contribution to this task with the use of so-called dynamic neural networks (LF8, HNN, and LRN) which considered the history of input parameters. The focus has been put on continuous time series rather than single solar SEP events. The new approach used here was the pre-processing of the input data. To characterise the solar flares and CMEs, special measures have been introduced as quantities characterising one-day-period intervals.

The successful and reliable forecast of SEP events can be a complicated enterprise. The approach undertaken in this work can be beneficial for SEP modellers and forecasters. For future work the questions arise: How much more additional information needs to be

This is the author's version of a manuscript that was accepted for publication in *Acta Astronautica*.

The definitive version was subsequently published in:

Fridrich Valach, Miloš Revallo, Pavel Hejda, and Josef Bochníček: Predictions of SEP events by means of a linear filter and layer-recurrent neural network.

Acta Astronautica, Volume 69, Issue 9-10, November 2011, Pages 758-766. DOI:10.1016/j.actaastro.2011.06.003

considered to improve the forecast? Is it even possible to improve forecasts using the scheme proposed in the underlying study? The questions will be left for future research investigations to answer.

Acknowledgements

This work was supported in part by VEGA grants 2/0015/11 and 2/0022/11 of the Scientific Grant Agency of the Ministry of Education of the Slovak Republic and the Slovak Academy of Sciences, by the Grant Agency of the ASCR under project IAA300120608 and by the Ministry of Education, Youth and Sports of the Czech Republic under project OC09070. The results presented in this paper rely on data collected and distributed by several institutions. The CME catalogue is generated and maintained at the CDAW Data Center by NASA and The Catholic University of America in cooperation with the Naval Research Laboratory. SOHO is a cooperative project of international of the ESA and NASA. The data on solar events were obtained from the NOAA Space Weather Prediction Center, Boulder, Colorado, USA and HEPF data from OMNIWeb operated by Space Physics Data Facility, NASA Goddard Space Flight Center, Greenbelt, Maryland, USA. The authors wish to thank the anonymous referees, whose valuable comments and suggestions helped to improve the quality of this paper.

References

- [1] J. Hwang, K.S. Cho, Y.J. Moon, R.S. Kim, Y.D. Park, Solar proton events during the solar cycle 23 and their association with CME parameters, *Acta Astronautica* 67 (2010) 353–361.
- [2] A.J. Tylka, J.H. Adams Jr., P.R. Boberg, B. Brownstein, W.F. Dietrich, E.O. Flueckinger, E.L. Petersen, M.A. Shea, D.F. Smart, E.C. Smith, CREME96: a revision of the cosmic ray effects on micro-electronics code. *IEEE Transactions on Nuclear Science* 44 (1997) 2150–2160.
- [3] N. Gopalswamy, A global picture of CMEs in the inner heliosphere, in: G. Poletto, S. T. Suess (Eds.), *The Sun and Heliosphere as an Integrated System*, ISBN 1-4020-2830-X (HB); ISBN 1-4020-2831-8 (e-book). *Astrophysics and Space Science Library*, Volume 317, Kluwer Academic Publishers, Dordrecht, The Netherlands, 2004, pp.201–251.
- [4] N. Gopalswamy, S. Yashiro, G. Michalek, G. Stenborg, A. Vourlidas, S. Freeland, R. Howard, *The SOHO/LASCO CME Catalog*, *EARTH MOON AND PLANETS* 104 (2009) 295-313. ISSN: 0167-9295, doi: 10.1007/s11038-008-9282-7.
- [5] T.G. Forbes, J.A. Linker, J. Chen, C. Cid, K. Kota, M.A. Lee, G. Mann, Z. Mikic, M.S. Potgieter, J.M. Schmidt, G.L. Siscoe, R. Vainio, S.K. Antiochos, P. Riley, CME theory and models. *Space Science Reviews* 123 (2006) 251-302.
- [6] M. Dryer, Comments on the origins of coronal mass ejections, *Solar Phys.* 169 (1996) 421–429.
- [7] A.J. Hundhausen, *Coronal Mass Ejections*, in: K.T. Strong, J.L.R. Saba, B.M. Haisch, J.T. Schmelz (Eds.), *The many faces of the sun : a summary of the results from NASA's Solar Maximum Mission*, Springer-Verlag, New York, 1999, p. 143.

This is the author's version of a manuscript that was accepted for publication in *Acta Astronautica*.

The definitive version was subsequently published in:

Fridrich Valach, Miloš Revallo, Pavel Hejda, and Josef Bochníček: Predictions of SEP events by means of a linear filter and layer-recurrent neural network.

Acta Astronautica, Volume 69, Issue 9-10, November 2011, Pages 758-766. DOI:10.1016/j.actaastro.2011.06.003

[8] R.A. Harrison, The nature of solar flares associated with coronal mass ejection, *Astron. Astrophys.* 304 (1995) 585–594.

[9] J. Zhang, K.P. Dere, R.A. Howard, M.R. Kundu, S.M. White, On the Temporal Relationship between Coronal Mass Ejections and Flares, *Asrophys. J.* 559 (2001) 452–462, doi:10.1086/322405

[10] D. Lario, Advances in modeling gradual solar energetic particle events, *Advances in Space Research* 36 (2005) 2279-2288.

[11] G.M. Simnett, Energetic Particles and Coronal Mass Ejections: a Case Study From ace and Ulysses, *Solar Phys.* 213 (2003) 387–412.

[12] D.V. Reames: Solar energetic particle variations, *Advances in Space Research* 34 (2004) 381–390.

[13] R. Schwenn, Space Weather: The Solar Perspective, *Living Rev. Solar Phys.*, 3, (2006), 2. [Online Article]: cited [28 October 2010], <http://www.livingreviews.org/lrsp-2006-2>

[14] A. Belov, Properties of solar X-ray flares and proton event forecasting. *Advances in Space Research* 43 (2009) 467–473, doi:10.1016/j.asr.2008.08.011

[15] J. Bochníček, P. Hejda, F. Valach, Solar energetic events in the years 1996–2004. The analysis of their geoeffectiveness, *Stud. Geophys. Geod.* 51 (2007) 439–447.

[16] F. Valach, P. Hejda, J. Bochníček, Geoeffectiveness of XRA events associated with RSP II and/or RSP IV estimated using the artificial neural network, *Stud. Geophys. Geod.* 51 (2007) 551–562.

This is the author's version of a manuscript that was accepted for publication in *Acta Astronautica*.

The definitive version was subsequently published in:

Fridrich Valach, Miloš Revallo, Pavel Hejda, and Josef Bochníček: Predictions of SEP events by means of a linear filter and layer-recurrent neural network.

Acta Astronautica, Volume 69, Issue 9-10, November 2011, Pages 758-766. DOI:10.1016/j.actaastro.2011.06.003

[17] N. Gopalswamy, S. Yashiro, A. Lara, M.L. Kaiser, B.J. Thompson, P.T. Gallagher, R.A. Howard, Large solar energetic particle events of cycle 23: A global view, *Geophys. Res. Lett.* 30 (12) (2003) 8015, doi:10.1029/2002GL016435.

[18] N. Gopalswamy, S. Yashiro, S. Krucker, G. Stenborg, R.A. Howard, Intensity variation of large solar energetic particle events associated with coronal mass ejections, *J. Geophys. Res.* 109 (2004) A12105, doi:10.1029/2004JA010602.

[19] Y.-J. Moon, K.-S. Cho, M. Dryer, Y.-H. Kim, Su-chan Bong, Jongchul Chae, Y.D. Park, New geoeffective parameters of very fast halo coronal mass ejections, *Astrophys. J.* 624 (2005) 414.

[20] P. Jiggins, S. Gabriel, D. Heynderickx, N. Crosby, A. Glover, Solar Energetic Particle Event (Sepe) Waiting Time Analysis as Part of the Sepem Project (Abstract), Abstract Book: 7th European Space Weather Week, Bruges, Belgium, November 15–19, 2010, p. 69.

[21] K. Gurney, *An Introduction to Neural Networks*, First published in 1997 by UCL Press, Reprinted 1999 by UCL Press, London, ISBNs: 1-85728-673-1, 1-85728-503-4.

[22] H. Demuth, M. Beale, M. Hagan, *Neural Network Toolbox 5, User's Guide*, The MathWorks, Natick 2005-2007.

[23] <http://cdaw.gsfc.nasa.gov/CME_list/> [Citation date: 05/10/2010].

[24] A. Bruzek, C.J. Durrant (Eds.), *Illustrated Glossary for Solar and Solar-Terrestrial Physics*, Freiberg, D. Reidel Publishing Company, Dordrecht, 1977.

[25] <<http://www.swpc.noaa.gov/ftpmenu/indices/events.html>> [Citation date: 20/05/2011]

[26] <<http://www.swpc.noaa.gov/ftpmenu/lists/ace.html>> [Citation date: 29/03/2011].

This is the author's version of a manuscript that was accepted for publication in *Acta Astronautica*.

The definitive version was subsequently published in:

Fridrich Valach, Miloš Revallo, Pavel Hejda, and Josef Bochníček: Predictions of SEP events by means of a linear filter and layer-recurrent neural network.

Acta Astronautica, Volume 69, Issue 9-10, November 2011, Pages 758-766. DOI:10.1016/j.actaastro.2011.06.003

[27] <<http://www.swpc.noaa.gov/ftpmenu/warehouse.html>> [Citation date: 20/05/2011].

[28] M. D. Schmid, A neural network package for Octave, User's Guide, Version: 0.1.9.1, 2009, <http://plexso.com/61_octave/neuralNetworkPackageForOctaveUsersGu.pdf> [Citation date: 05/10/2010].

[29] S.W. Kahler, E.W. Cliver, A.G. Ling, Validating the proton prediction system (PPS), *Journal of Atmospheric and Solar-Terrestrial Physics* 69 (2007) 43–49.

Table 1. Comparison of neural-network models performances for several chosen critical HEPF levels. (HEPF are given in pfu = particles/cm².s.sr). Statistics of alerts announced following Recipes A and B, respectively, and using four NN models are compared. All together 754 forecasts were carried out during the test period 13/08/2003 – 26/11/2005. During this interval, the thresholds for SEP events fixed at 100 pfu, 200 pfu, 500 pfu, and 1000 pfu were exceeded for 34, 19, 12, and 11 days, respectively.

Recipe	[pfu]Critical level of HEPF	Model	A safety measure was performed				No safety measure was performed			Hanssen-Kuiper skill score
			SEP event occurred (Hits)	SEP event did not occur (False alarms)	Days with SEP events [%]	Days when safety measure was performed [%]	SEP event occurred (Missing alerts)	SEP event did not occur (Correct non-events)	Days with SEP events [%]	
A	100	LF0	21	77	21.5	13.0	13	645	1.98	0.51
		LF8	18	199	8.3	28.7	16	523	2.97	0.25
		HNN	4	19	17.4	3.0	30	703	4.09	0.09
		RNN	18	33	35.3	6.7	16	689	2.27	0.48
	200	LF0	12	52	18.7	8.5	7	685	1.01	0.56
		LF8	13	121	9.7	17.7	6	616	0.96	0.52
		HNN	3	13	18.7	2.1	16	724	2.16	0.14
		RNN	8	11	42.1	2.5	11	726	1.49	0.41
	500	LF0	5	19	20.8	3.2	7	725	0.96	0.39
		LF8	5	49	9.3	7.1	7	695	1.00	0.35
		HNN	1	12	7.7	1.7	11	732	1.48	0.07
		RNN	0	0	---	0.0	12	744	1.59	0.00
	1000	LF0	2	6	25.0	1.1	9	739	1.20	0.17
		LF8	0	8	0	1.1	11	737	1.47	-0.01
		HNN	1	11	8.3	1.6	10	734	1.34	0.08
		RNN	0	0	---	0.0	11	745	1.45	0.00
B	100	LF0	29	142	17.0	22.6	5	580	0.85	0.66
		LF8	28	278	9.1	40.5	6	444	1.33	0.44
		HNN	19	44	30.2	8.3	15	678	2.16	0.50
		RNN	26	61	29.9	11.5	8	661	1.20	0.68
	200	LF0	18	94	16.1	14.8	1	643	0.15	0.82

This is the author's version of a manuscript that was accepted for publication in *Acta Astronautica*.

The definitive version was subsequently published in:

Fridrich Valach, Miloš Revallo, Pavel Hejda, and Josef Bochníček: Predictions of SEP events by means of a linear filter and layer-recurrent neural network.

Acta Astronautica, Volume 69, Issue 9-10, November 2011, Pages 758-766. DOI:10.1016/j.actaastro.2011.06.003

	LF8	18	176	9.3	25.7	1	561	0.18	0.71
	HNN	12	28	30.0	5.3	7	709	0.98	0.59
	RNN	14	25	35.9	5.2	5	712	0.70	0.70
500	LF0	9	40	18.4	6.5	3	704	0.42	0.70
	LF8	11	79	12.2	11.9	1	665	0.15	0.81
	HNN	8	24	25.0	4.2	4	720	0.55	0.63
	RNN	6	6	50.0	1.6	6	738	0.81	0.49
1000	LF0	6	17	26.1	3.0	5	728	0.68	0.52
	LF8	5	20	20.0	3.3	6	725	0.82	0.43
	HNN	7	22	24.1	3.8	4	723	0.55	0.61
	RNN	5	6	45.5	1.5	6	739	0.80	0.45

Table 2. Comparison of combined LF0-RNN model performances for several chosen critical HEPF levels. (HEPF are given in pfu = particles/cm².s.sr). Statistics of alerts announced following Recipes A and B, respectively.

Recipe	[pfu]Critical level of HEPF	A safety measure was performed			[%]Days when safety measure was performed	No safety measure was performed			Hanssen-Kuiper skill score
		SEP event occurred (Hits)	SEP event did not occur (False alarms)	Days with SEP events [%]		SEP event occurred (Missing alerts)	SEP event did not occur (Correct non-events)	Days with SEP events [%]	
A	100	20	63	24.1	11.0	14	659	2.08	0.50
	200	12	29	29.3	5.4	7	708	0.98	0.59
	500	2	10	16.7	1.6	10	734	1.34	0.15
	1000	0	0	---	0.0	11	745	1.46	0.00
B	100	28	116	19.4	19.0	6	606	0.98	0.66
	200	18	59	23.4	10.2	1	678	0.15	0.87
	500	9	23	28.1	4.2	3	721	0.41	0.72
	1000	5	6	45.5	1.5	6	739	0.81	0.45

This is the author's version of a manuscript that was accepted for publication in *Acta Astronautica*.

The definitive version was subsequently published in:

Fridrich Valach, Miloš Revallo, Pavel Hejda, and Josef Bochníček: Predictions of SEP events by means of a linear filter and layer-recurrent neural network.

Acta Astronautica, Volume 69, Issue 9-10, November 2011, Pages 758-766. DOI:10.1016/j.actaastro.2011.06.003

The captions of the figures:

Figure 1

Time series of SEP fluxes for the final test (13/08/2003 – 26/11/2005). Observed values are compared with those obtained as predictions of the linear filter (LF0) as well as with those modelled by the recurrent network (RNN). (Note: Some interesting parts of these series are shown in more detail on Figure 2).

Figure 2

Detailed views of some parts of the test time series of SEP fluxes when there were increased values of HEPF > 10 MeV. The SEP fluxes modelled by the linear filter (LF0) as well as with the recurrent network are compared with the observed fluxes. The subplots in the figure depict the time series on about 28/02/2003 (a), 27/07/2004 (b), 13/09/2004 (c), 10/11/2004 (d), 17/01/2005 (e), 15/05/2005 (f), 15/07/2005 (g), and 11/09/2005 (h), respectively. The legend of the pictures is given in the right bottom panel.

Figure 1

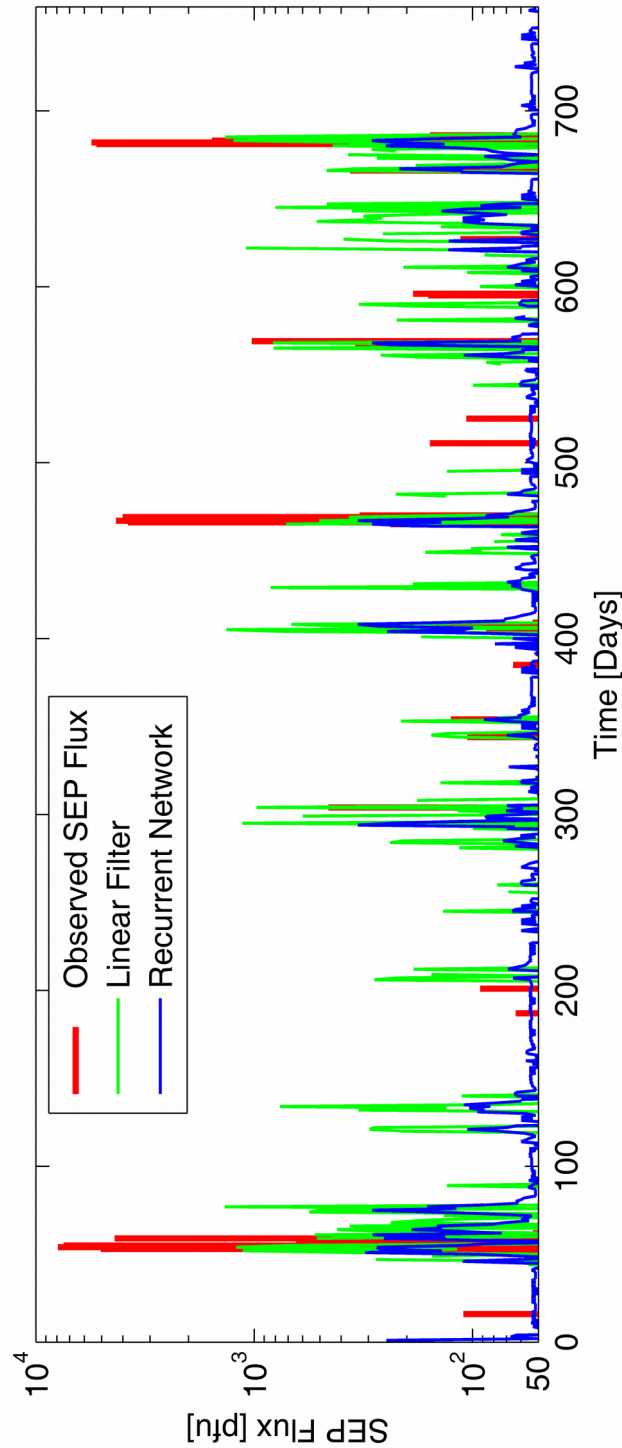


Figure 2

